Journal of Bio- and Tribo-Corrosion (2020) 6:29
https://doi.org/10.1007/s40735-020-0323-8

Effect of Mixed-Ligands Copper Complex on the Corrosion Inhibition of Carbon Steel in Sulfuric Acid Solution

R. N. El-Tabesh[1] · A. M. Abdel-Gaber[1,2] · H. H. Hammud[3] · R. Oweini[1,4]

Received: 18 September 2019 / Revised: 29 November 2019 / Accepted: 21 January 2020 / Published online: 31 January 2020

Abstract
The effect of Bis-phenanthroline chloro copper(II) chloride di-para-aminobenzoic acid tetrahydrate complex $[Cu(Phen)_2Cl]Cl\ (pABz)_2{\cdot}4H_2O$, CuPAB, on the corrosion behavior of carbon steel in 0.5 M sulfuric acid solutions were studied by electrochemical impedance spectroscopy (EIS), and potentiodynamic polarization techniques. The shift of corrosion potential and the variation in the anodic Tafel line slope values, obtained from polarization measurements, indicated that CuPAB acts as a mixed-type inhibitor. Impedance suggests that inhibition of the complex is assisted by their adsorption at the metal/solution interface. Theoretical fitting of different adsorption isotherms such as Langmuir, Flory–Huggins, and the kinetic–thermodynamic models has been tested. The adsorption isotherm parameters indicate that the adsorption behavior of complex on the metal surface is not ideal. The high binding constant of CuPAB showed a stronger interaction between the metal surface and the complex. The obtained data revealed that CuPAB complex has remarkable inhibiting effects on the corrosion of steel in 0.5 M H_2SO_4. Spectrophotometry measurements were employed to investigate the stability of the complex in acidic media. The thermodynamic activation parameters were calculated. The data explained that the inhibition takes place through the adsorption that is neither physical nor chemical but a combination of both (physicochemical).

Keywords Acid solutions · Carbon steel · Sulfuric acid · EIS · Polarization · Acid inhibition

1 Introduction

Steel is extensively utilized in store tanks, petroleum refineries, and many industries. Acid solutions are widely used for removal of scale and rust in many industrial processes [1–3]. Inhibitors are usually used to reduce the corrosive attack on metallic materials by acid solutions. The majority of the well-known acid inhibitors are organic compounds with nitrogen, sulfur, and oxygen. Inhibitors act on the metal/solution interface through adsorption. This phenomenon could be achieved through (i) electrostatic attraction between the metal and the inhibitor molecules, (ii) interaction between the unshared lone electron pairs of the inhibitor and the *d*-orbital of the metal, (iii) π-electron ligand–metal interaction, and (iv) combination of all [4]. If the adsorption process involves overlaping of filled ligand non-bonding orbital with metal empty inner *d* or *f* orbital, a coordinate-type bond formed and the process is termed chemisorption [5]. This situation occurs in cases where the inhibitor molecules contain lone pairs of electrons, multiple bonds, or conjugated π-type bond system [6–8]. 1,10-Phenanthroline is a tricyclic aromatic bidentate *N*, *N*-heterocyclic ligand known to form strong chelate complexes with most metal ions [9]. It acts as a predominantly cathodic corrosion inhibitor for mild steel in H_2SO_4 solutions [10] and as a mixed-type inhibitor in HCl and chloride containing solutions [11–14]. As a strong complexing ligand, chemisorption on the metal surface via the electron donor properties of nitrogen atoms as well as π-electron of aromatic ring has also been suggested [15]. Phenanthroline could also form insoluble metal complexes that further inhibit corrosion on the surface of the metal. However, there are few reports about the corrosion inhibition

✉ A. M. Abdel-Gaber
ashrafmoustafa@yahoo.com

[1] Department of Chemistry, Faculty of Science, Beirut Arab University, Beirut, Lebanon

[2] Department of Chemistry, Faculty of Science, Alexandria University, Ibrahimia, P.O. Box 426, Alexandria 21321, Egypt

[3] Chemistry Department, Faculty of Science, King Faisal University, Al-Ahsa 31982, Saudi Arabia

[4] KAS Central Research Science Laboratory, FAS, American University of Beirut, Beirut, Lebanon

for its metal complexes. Phenanthroline derivatives in acidic media act as efficient corrosion inhibitors for steel [16, 17]. Metal complexes may also act as corrosion inhibitors. Co(II), Zn(II), Mn(II) acetylacetonate complexes show corrosion inhibitive performance for mild steel in 3.5% NaCl solution. This is supported by SEM–EDX analysis, which showed the precipitation or film formation of the metallic complexes on the mild steel surface [18]. Two phenolic Schiff base ligands, 4EMP and 4NMP were investigated as corrosion inhibitors on mild steel surface in 1 M HCl solution. The results of the electrochemical methods showed that the studied molecules imparted high resistance in allowing the flow of electrons across the metal–electrolyte platform and behaved as mixed-type inhibitors [19]. The inhibitory effect of schiff base Salpr and its stable octahedral cobalt complex is due to their adsorption over the steel surface as investigated by electrochemical impedance spectroscopy (EIS) and potentiodynamic polarization techniques [20]. Two new eco-friendly Schiff base metal complexes of Cr and Co were evaluated as corrosion inhibitors against carbon steel dissolution in 1 M H_2SO_4 using electrochemical and quantum chemical studies. The results state that the two complexes acted as mixed-type inhibitors. The degree of surface coverage values obeyed the Langmuir adsorption [21]. Zinc acetate/Urtica Dioica hybrid green corrosion inhibitive complex showed effective inhibition action in saline solution on carbon steel. The synergistic effect between Zn^{2+} cations and inhibitive compounds existed in Urtica Dioica, which resulted in protective film deposition on the steel surface [22]. Cobalt phenanthroline complex showed a greater inhibiting effect than its ligand phenanthroline on carbon steel in sulfuric acid [23].

The aim of the present work is to study the effect of Bis-phenanthroline chloro copper(II) chloride di-para-aminobenzoic acid tetrahydrate, CuPAB, on the corrosion behavior of carbon steel in 0.5 M sulfuric acid solution.

2 Experimental

2.1 Materials Preparation

Bis-phenanthroline chloro copper(II) chloride di-para-aminobenzoic acid tetrahydrate $[Cu(Phen)_2Cl]Cl\ (pABz)_2{\cdot}4H_2O$, CuPAB, was synthesized by the reaction of equimolar of each of p-amino benzoic acid, phenanthroline, and $CuCl_2{\cdot}2H_2O$ in methanol at room temperature [24]. The used reagents 1,10-phenanthroline and para-amino benzoic acid were purchased from Aldrich Chemical company.

2.2 Solution Preparation

All chemicals used in this study, namely, sulfuric acid and absolute ethanol (Riedel-de Haen, 99.8%) were reagent grade. A Stock solution of 10–2 M CuPAB was prepared by dissolving the appropriate weight of CuPAB in absolute ethyl alcohol. The test solution containing 10% ethanol was prepared by diluting the stock solution and the appropriate volume of 4 M H_2SO_4 using ethanol and distilled water. Any test solution used during the study contains 10% ethanol.

2.3 Electrochemical Measurements

EIS and polarization curve measurements were performed using a frequency response analyzer (FRA)/potentiostat supplied from ACM instruments (UK). Experiments were carried out using a conventional three electrode cell assembly with a platinum sheet counter electrode and a saturated calomel electrode (SCE) as auxiliary and reference electrodes. The carbon steel with the following chemical composition (wt%) C, 0.164; S, 0.001; Mn, 0.710; P, 0.0005; Si, 0.26, Ni, 0.123; Cr, 0.041; balance Fe was used for constructing the working electrode. Carbon steel rod of cylindrical shape was encapsulated in Teflon in such a way that only one surface was left uncovered. The exposed area (1.0 cm^2) was abraded by a series of emery papers of variable grades, starting with a coarse one and proceeding to the finest (800) grade. The frequency range of EIS measurements was $0.1–96 \times 10^3$ Hz with a signal amplitude perturbation of 10 mV around the corrosion potential. Each experiment was conducted at least twice in order to achieve good reproducibility. Measurements of polarization curves were obtained by automatically polarizing the working electrode from ± 250 mV versus the rest potential with a scanning rate of 60 mV/min. All tests were performed at 30 ± 0.10.

2.4 UV–Vis Spectrophotometry

Ultraviolet–visible (UV–VIS) spectrophotometry was conducted on a Jasco V630 Spectrophotometer.

3 Results and Discussion

3.1 Potentiodynamic Polarization Measurements

Inspection of the polarization curves, Fig. 1, suggests that the addition of CuPAB retards both metal dissolution and hydrogen evolution reactions. The inhibitory effect of the

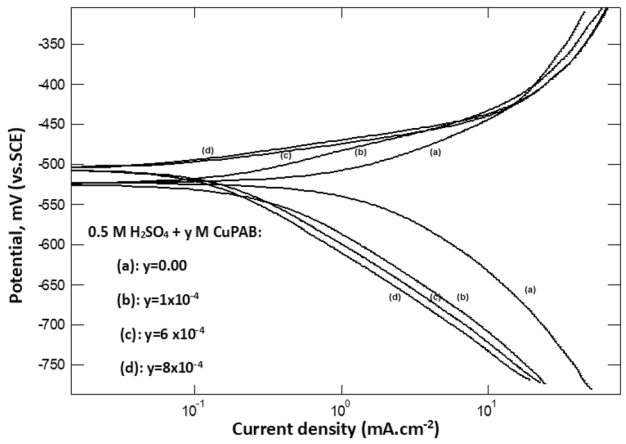

Fig. 1 Potentiodynamic polarization curves for carbon steel in 0.5 M sulfuric acid solution in the absence and presence of different concentrations of CuPAB at 30 °C

CuPAB could therefore be attributed to the blockage of the anodic and cathodic sites on the metal surface indicating that CuPAB acts as a mixed-type inhibitor.

The electrochemical polarization parameters obtained for different CuPAB concentrations are shown in Table 1. The inhibition efficiency ($\%\eta$) was calculated using the relation

$$\%h = \left[\left(i_{\text{corr}} - i_{\text{corr(inh)}}\right)/i_{\text{corr}}\right] \times 100,$$

where i_{corr} and $i_{\text{corr(inh)}}$ represent the corrosion current density values free from and containing CuPAB, respectively. The data showed that as the concentration of CuPAB increases, the inhibition efficiency increases. It is clear that E_{corr} value was shifted towards less negative potential (anodic direction). It has been reported that a compound can be classified as an anodic or a cathodic-type inhibitor based on shift in E_{corr} value [25]. If the shift in E_{corr} is greater than 85 mV, towards anode or cathode with reference to blank, then an inhibitor is classified as either anodic- or cathodic-type inhibitor. Otherwise, inhibitor is treated as a mixed type [26]. The maximum displacement in E_{corr}, in this study, value was around 64 mV indicating that CuPAB acts as a mixed-type inhibitor.

Table 1 The electrochemical polarization parameters for carbon steel in 0.5 M sulfuric acid solution in the absence and presence of different concentrations of CuPAB at 30 °C

Conc. (mol L^{-1})	E_{corr} (mV vs. SCE)	β_a (mV decade^{-1})	β_c	i_{corr} (mA cm^{-2})	$\%\eta$
0.0	517	122	80	1.20	–
1×10^{-5}	524	75	116	1.09	9.2
8×10^{-5}	530	70	113	0.83	30.8
1×10^{-4}	516	48	109	0.22	81.6
6×10^{-4}	524	49	108	0.20	83.3
8×10^{-4}	501	32	117	0.11	90.8
1×10^{-3}	453	29	120	0.10	91.6

The Tafel slope provides insight into the reaction mechanism and can be used to evaluate the rate-determining steps, which generally assume extreme coverage of the adsorbed species. The Tafel slope dependence on coverage provides the fundamental understanding of the potential-dependent shift in the Tafel slopes [27]. The change of the anodic Tafel slopes (β_a) with the addition of inhibitors suggests that the inhibitors were first adsorbed onto the metal surface and impede the passage of metal ions from the metal surface into the solution, by blocking the reaction sites of the metal surface thus affecting the anodic reaction mechanism [28]. Moreover, the variation in the β_a values is more than that in the β_c values, indicating that the more inhibition effect of CuPAB on the anodic process than on the cathodic process [29].

3.2 Electrochemical Impedance Spectroscopy (EIS) Measurements

Figure 2 shows that the Nyquist impedance plots for carbon steel in 0.5 M sulfuric acid (insert) consisted of two depressed capacitive semicircles. These depressed semicircles are followed by an inductive loop located at the low-frequency region in the presence of CuPAB complex. The inductive loop is often attributed to either species relaxation like $FeSO_4$ or inhibitor species on the electrode surface [30].

Figure 3 shows the experimental and computer fit results as well the equivalent circuit models of Nyquist plots of 0.5 M H_2SO_4 (a) and 0.5 M H_2SO_4 in the presence of 1×10^{-3} M of CuPAB (b). The equivalent circuit presented on the inset of Fig. 3a consists of two circuits connected

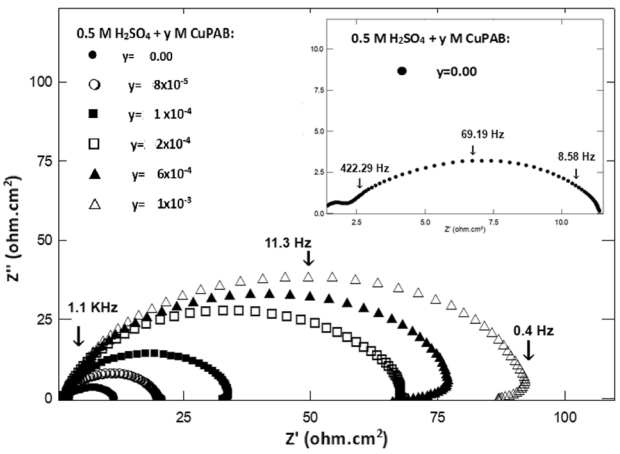

Fig. 2 Nyquist impedance plots for carbon steel in 0.5 M sulfuric acid in the absence and presence of different concentrations of CuPAB

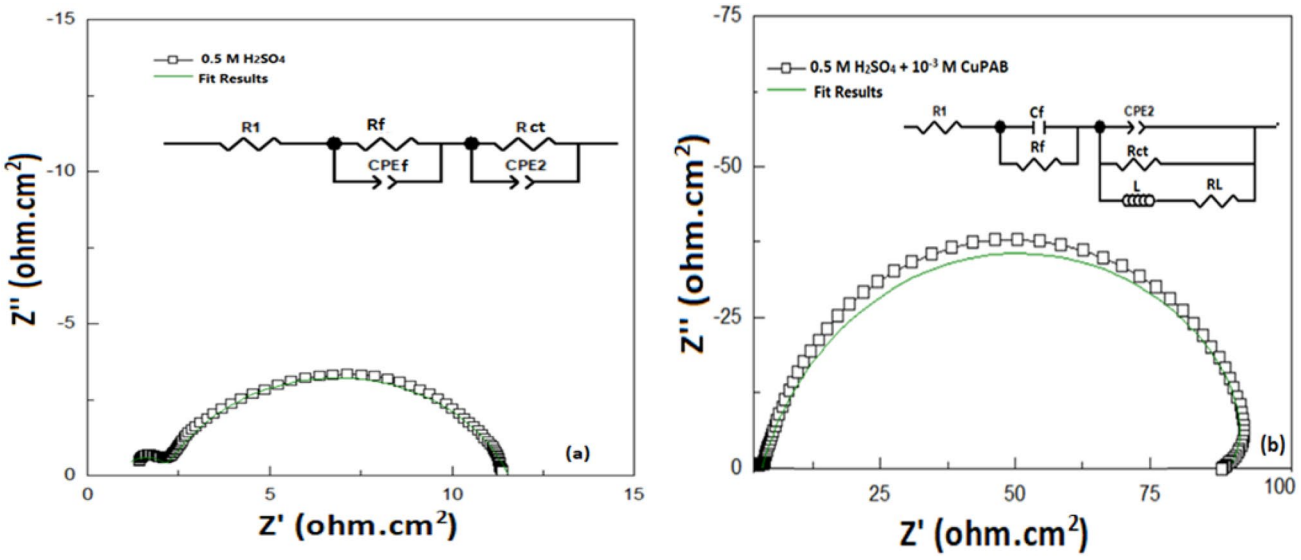

Fig. 3 The experimental and computer fit results as well the equivalent circuit models of Nyquist impedance plot for carbon steel in 0.5 M H_2SO_4 (**a**) and 0.5 M H_2SO_4 in the presence of 1×10^{-3} M of CuPAB (**b**)

in series, and includes the solution resistance (R_s) and the constant phase element (CPE) which is placed in parallel to charge transfer resistance element (R_{ct}). The CPE is defined by two values, the non-ideal double layer capacitance (Q_{dl}) and a constant (n). For a non-homogeneous system, n values range from 0.9 to 1, as well as the film resistance R_f and the corresponding capacitance CPE_f. On the other hand, the equivalent circuit presented on the inset of Fig. 3b comprises an ideal film capacitance C_f parallel to R_f as well as an inductive resistance (R_L) and an inductance L. The fitting of the spectrum to the equivalent circuit models allows the evolution of the elements of the circuit analogue.

The impedance, Z, of CPE is presented by

$$Z_{CPE} = Q^{-1}(i\omega)^{-n},$$

where $i=(-1)^{1/2}$, ω is the frequency in rad s^{-1}, $\omega=2\Pi f$, and f is the frequency in Hz. If n equals 1, the value of Q present in the above equation is identical to that of ideal capacitor C, since $Z_{CPE}=(i\omega C)^{-1}$. In this case, the Q that is equal to C has units of capacitance, i.e., μF/cm^2, and represents the double layer capacitance of the interface. However, for a non-homogeneous system, where n values are different from 1, Q is equal to the CPE admittance (Y_0) and has units of $\mu s^n/\Omega\ cm^2$. The double layer capacitance (C_{dl}) in μF/cm^2 could be calculated using the following equation [31–33].

$$C_{dl} = \frac{(Y_0 \cdot R_{ct})^{1/n}}{R_{ct}}$$

The fitting of the spectrum to the equivalent circuit models allows the evolution of the elements of the circuit analogue.

The inhibition efficiency (%η) was calculated from impedance measurements using the relation:

$$\%h = \left[\left(R_{ct}-R_{ct0}\right)/R_{ct}\right] \times 100,$$

where R_{ct0} and R_{ct} represent the charge transfer resistance free from and containing inhibitor, respectively.

Inspection of Table 2 reveals that R_{ct} value increases and Q_{dl} decreases in the presence of CuPAB complex. This can be explained on the basis of the Helmholtz model [34], the

Table 2 Eelectrochemical impedance parameters for carbon steel in 0.5 M H_2SO_4 acid in the absence and presence of different concentrations of CuPAB at 30 °C

Conc., mol L^{-1}	R_s Ω cm^2	C_f μF/cm^2	R_f Ω cm^2	R_{ct} Ω cm^2	$Y_0=Q$ $\mu s^n/\Omega\ cm^2$	N	C_{dl} μF/cm^2	L Henri cm^2	R_L Ω cm^2	%η
0.0	1.54	1.56	2.30	9	6500	0.83	3640	–	–	–
8×10^{-5}	0.89	1.97	1.02	19	509	0.81	1710	7	385	53
1×10^{-4}	0.73	1.92	1.05	33	253	0.87	1230	328	900	73
2×10^{-4}	0.83	1.86	1.04	67	202	0.88	112	560	1205	87
6×10^{-4}	0.83	1.89	1.03	76	200	0.85	95.5	613	1230	88
1×10^{-3}	0.66	2.01	1.14	91	176	0.87	94.8	1123	2070	90

Table 3 Linear fitting parameters of the experimental data to Langmuir, Kinetic–thermodynamic model, and Florry–Huggins

Inhibitor	Langmuir		Kinetic–thermodynamic			Florry–Huggins		
	K	R^2	K	$1/y$	R^2	K	x	R^2
CuPAB	–	–	8910	0.95	0.97	8688	0.83	0.91

decrease in Q_{dl} can result from a decrease in local dielectric constant and/or an increase in the thickness of the electrical double layer, suggesting that inhibition by molecules is assisted by their adsorption at the metal/solution interface [35].

The slight difference of $\%\eta$, obtained from impedance and polarization, could result from the variation of Tafel lines slopes (β_a, β_c) with increasing CuPAB concentrations [36]. In impedance measurements, the rate of corrosion is taken as the reciprocal of the charge transfer resistance. This approximation is based on the assumption that the cathodic and anodic Tafel slopes within the concentration under study are constant [34]. In an activation controlled system, the corrosion current density (i_{corr}) could be calculated using Stern–Geary equation [37]:

$$i_{corr} = \frac{(\beta_a \cdot \beta_c)}{2 \cdot 303(\beta_a + \beta_c)} \cdot \frac{1}{R_{ct}}$$

Therefore, the %η obtained from polarization and impedance measurements will be in good agreement with each other only if the Tafel slopes remain constant with increasing CuPAB concentration.

3.3 Adsorption Consideration

The degrees of surface coverage values ($\theta = \%\eta/100$) were obtained from potentiodynamic polarization measurements. Table 3 shows the fitting parameters of the experimental data to Langmuir, Kinetic–thermodynamic model, and Florry–Huggins [38–40].

The poor correlation between CuPAB and Langmuir adsorption isotherm indicates that the adsorption behavior of complex on the metal surface is not ideal. The number of active sites occupied by a single inhibitor molecule, $1/y$, was equivalent to the number of absorbed water molecules (x) replaced by a given CuPAB molecule. This indicates that the complex and water molecule are of similar size [41]. The high binding constant K of CuPAB shows a stronger interaction between the metal surface and CuPAB in sulfuric acid media.

3.4 Activation Parameters

Figure 4 indicates that increasing temperature affects both cathodic hydrogen evolution and anodic carbon steel

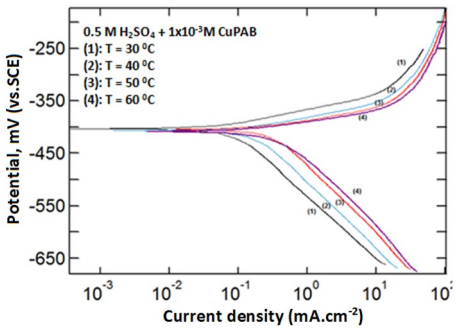

Fig. 4 Potentiodynamic polarization curves for carbon steel in 0.5 M H_2SO_4 in the presence of 1×10^{-3} M of CuPAB at different temperatures

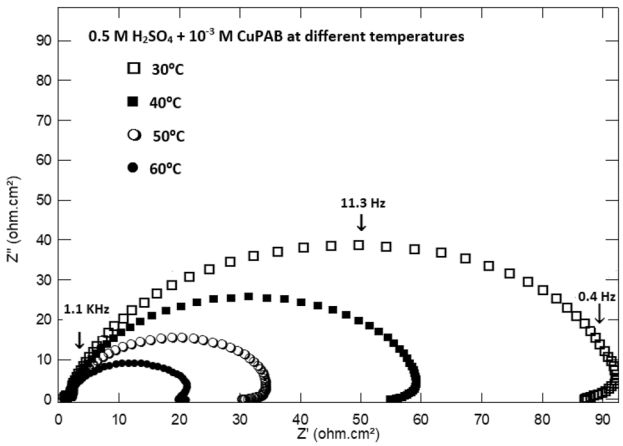

Fig. 5 Nyquist impedance plots for carbon steel in 0.5 M H_2SO_4 in the presence of 1×10^{-3} M of CuPAB at different temperatures

dissolution processes in 0.5 M H_2SO_4 in the presence of 1×10^{-3} M of CuPAB.

The corresponding Nyquist impedance plots are shown in Fig. 5. It is clear that increasing temperature decreases the size of the depressed semicircles and hence increases the corrosion rate for CuPAB.

The ΔE*, ΔH*, and ΔS* thermodynamic parameters were obtained from the graphical representation of Arrhenius and transition state equations [42]. Figures 6 and 7 show the linear square fitting of ln(υ) and ln (υ/T) data vs. ($1/T$). The corrosion rate, υ, was taken as the corrosion current density obtained from the potentiodynamic polarization curves at different temperatures. The figures explain that

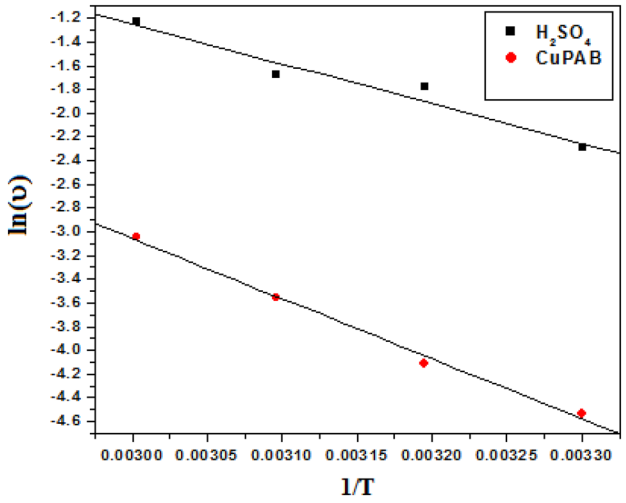

Fig. 6 Variation of ln(υ) with 1/T of carbon steel in 0.5 M sulfuric acid solution in the absence and presence of the CuPAB

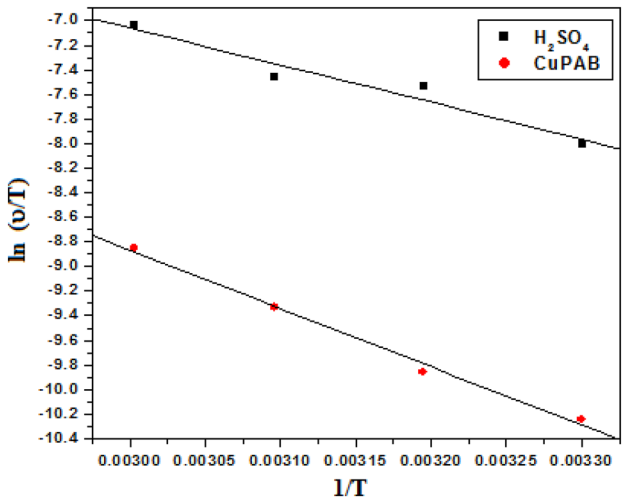

Fig. 7 Variation of ln(υ/T) with 1/T of carbon steel in 0.5 M sulfuric acid solution in the absence and presence of the CuPAB

the efficiency of CuPAB is reduced at higher temperatures. This indicates that the adsorption of the ligand and the corresponding complex decreases with increasing temperature. The change in the free energy of activation (ΔG*) was also calculated at 30 °C using the relation:

$$\Delta G* = \Delta H* - T\Delta S*$$

The activation parameters have been computed and shown in Table 4. The increase of ΔE* in the presence of inhibitors was attributed to the adsorption of CuPAB on the carbon steel surface. It could be concluded that the formation of the activated complex is an endothermic process since ΔH* has positive value, whereas the negative value of the entropy of activation, ΔS*, means a decrease in disorder [43, 44].

Table 4 Kinetic and adsorption parameters of carbon steel in 0.5 M H_2SO_4 in the absence and presence of 1×10^{-3}M CuPAB

Solution	ΔE* kJ mol^{-1}	ΔH* kJ mol^{-1}	ΔS* J mol^{-1} K^{-1}	ΔG_{ads} kJ mol^{-1}
H_2SO_4	27.7	25.2	−181	–
CuPAB	42.0	39.3	−153	−34.41

However, the standard free energy of adsorption (ΔG_{ads}) was calculated using the equation [45]:

$$K_{ads} = 1/55.5\, e^{(-\Delta G ads/RT)},$$

where R is the molar gas constant, T is the absolute temperature in Kelvin, and 55.5 is the concentration of water at the metal/solution interface expressed in molar. The value of K was obtained from the kinetic thermodynamic model. The negative values of the ΔG_{ads} in sulfuric acid indicate the spontaneity of the adsorption process. Since the value of ΔG_{ads} −34.41 for CuPAB lies between −20 and −40 kJ/mol, the adsorption of the inhibitor molecules on metal surface is attributed to physicochemical adsorption mechanism [46, 47]. The higher anticorrosion efficiency of metal complexes is due to the low water solubility, high molecular weight, and molecular planarity and stability of the complexes. In addition, CuPAB acted as a carrier of co-crystallized *p*-aminobenzoic acid to the surface of carbon steel. The latter can coordinate to dissolved iron ion at the carbon steel surface, forming a stable film hindering further iron dissolution and thus retarding corrosion.

3.5 Spectrophotometric

The UV–Vis spectrophotometry was used to monitor the stability of the CuPAB complex through observing the maximum absorbance and the corresponding wavelength over the period of the testing time. Several authors used this technique to study the stability of complexes in different media [48, 49]. The UV–Vis absorption spectra, Fig. 8, show an absorption band at 272 nm due to π–π* of coordinated phenanthroline ligand. The complex also shows an absorption shoulder at 300 nm due to *n*–π* of phenanthroline and p-aminobenzoate ligands. The absorption behavior for the CuPAB confirms that the complex is stable under ambient conditions in the acid solution over an hour as the UV–Vis spectra were not changed obviously in 60 min.

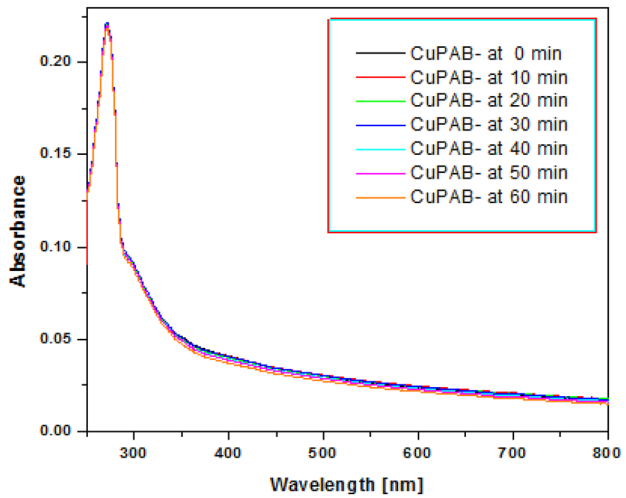

Fig. 8 UV–Vis absorption spectra for 1×10^{-4}M CuPAB in 0.5 M sulfuric acid solution recorded from 0 to 60 min at 30 °C

4 Conclusion

In the literature, there are only a few papers that investigate the use of mixed-ligand complexes as corrosion inhibitors. The stable CuPAB complex was found to be an efficient mixed-type inhibitor for corrosion of carbon steel in 0.5 M H_2SO_4 solutions. The high binding constant indicates its remarkable effect as corrosion inhibitor. The CuPAB complex can be present in both molecular and protonated species and its inhibitive effect was attributed to the adsorption over the metal surface via a combination of physical and chemical (physicochemical) adsorption process.

Acknowledgements The authors wish to thank Dr. H.T. Rahal for her effort in revising the manuscript.

Compliance with Ethical Standards

Conflict of interest On behalf of all authors, the corresponding author states that there is no conflict of interest.

References

1. Behpour M, Ghoreishi SM, Mohammadi N, Soltani N, Salavati-Niasari M (2010) Investigation of some Schiff base compounds containing disulfide bond as HCl corrosion inhibitors for mild steel. Corros Sci 52:4046
2. Rahal HT, Abdel-Gaber AM, Younes GO (2016) Inhibition of steel corrosion in nitric acid by sulfur containing compounds. Chem Eng Commun 203:435–445
3. Abdel-Gaber AM, Awad R, Rahal HT, Moussa D (2019) Electrochemical behavior of composite nanoparticles on the corrosion of mild steel in different media. J Bio Tribo Corros 5:49
4. Schweinsgberg D, George G, Nishihara H (1990) Adsorption and corrosion inhibition effect of polar organic compounds on iron in 1 M $HClO_4$ containing SH-. J Electrochem Soc 137:1354
5. Mansfeld F (1987) Corrosion mechanisms. Marcel Dekker Inc., New York
6. Hackerman N (1962) Recent advances in understanding of organic inhibitors. Corrosion 18:322
7. Nobe K, Eldakar N (1981) Effect of substituted benzotriazoles on the anodic dissolution of iron in H_2SO_4. Corrosion 37:271
8. El-Awady AA, Abd-El-Nabey BA, Aziz SG (1992) Kinetic-thermodynamic and adsorption isotherms analyses for the inhibition of the acid corrosion of steel by cyclic and open-chain amines. J Electrochem Soc 139:2150
9. Luman CR, Castellano FN (2003) Phenanthroline ligands. Comprehensive coordination chemistry II. Elsevier, Oxford
10. Banerjee SN, Misra S (1989) 1,10,-Phenanthroline as corrosion inhibitor for mild steel in sulfuric acid solution. Corrosion 45:780–783
11. El Ouafi A, Hammouti B, Oudda H, Kertit S, Benkaddour M, Ben-Hadda T (2002) Study of the inhibiting power of 2,9-chloromethyl-1,10-phenanthroline for the corrosion of mild steel in molar hydrochloric acid solution at 90 _C. Ann Chim Sci Mater 27:71–80
12. Mu GN, Li X, Li F (2004) Synergistic inhibition between o-phenanthroline and chloride ion on cold rolled steel corrosion in phosphoric acid. Mater Chem Phys 86:59–68
13. Li X, Tang L, Li L, Mu G, Liu G (2006) Synergistic inhibition between o-phenanthroline and chloride ion for steel corrosion in sulfuric acid. Corros Sci 48:308–321
14. Agarwala VS (1990) Corrosion inhibition by phenanthrolines. Corrosion 46:376–379
15. Schmid GM, Huang HJ (1980) Spectro-electrochemical studies of the inhibition effect of 4, 7-diphenyl-1,10-phenanthroline on the corrosion of 304 stainless steel. Corros Sci 20:1041–1057
16. Obot IB, Obi-Egbedi NO, Eseola AO (2011) Anticorrosion potential of 2-mesityl-1H-imidazo[4,5-f] [1, 10]-phenanthroline on mild steel in sulfuric acid solution: experimental and theoretical study. Ind Eng Chem Res 50:2098–2110
17. de la Luz Perez-Arredondo M, del Refugio Gonzalez-Ponce M, Ana Zanor G, Antonio Ramirez Vazquez J, Segoviano-Garfias JJN (2015) Complex formation equilibria of 2,2'-bipyridyl and 1,10-phenanthroline with manganese(II) in methanol. Karbala Int J Mod Sci 1:178–186
18. Mahdavian M, Attar MM (2009) Electrochemical behaviour of some transition metal acetylacetonate complexes as corrosion inhibitors for mild steel. Corros Sci 51:409–414
19. Elemike EE, Nwankwo HU, Onwudiwe DC, Hosten EC (2017) Synthesis, crystal structures, quantum chemical studies and corrosion inhibition potentials of 4-(((4-ethylphenyl)imino)methyl) phenol and (E)-4-((naphthalen-2-ylimino) methyl) phenol Schiff bases. J Mol Struct 1147:252–265
20. Abdel-Gaber AM, Masoud MS, Khalil EA, Shehata EE (2009) Electrochemical study on the effect of Schiff base and its cobalt complex on the acid corrosion of steel. Corros Sci 51(12):3021–3024
21. Zakaria K, Negm NA, Khamis EA, Badr EA (2016) Electrochemical and quantum chemical studies on carbon steel corrosion protection in 1 M H_2SO_4 using new eco-friendly Schiff base metal complexes. J Taiwan Inst Chem Eng 61:316–326
22. Salehi E, Naderi R, Ramezanzadeh B (2017) Synthesis and characterization of an effective organic/inorganic hybrid green corrosion inhibitive complex based on zinc acetate/Urtica Dioica. Appl Surf Sci 396:1499–1514
23. Liu X, Okafor PC, Jiang B, Hu H, Zheng Y (2015) Electrochemical study on the inhibition effect of phenanthroline and

its cobalt complex as corrosion inhibitors for mild steel. J Mater Eng Perform 24:3599–3606
24. El-Tabesh RN (2012) Synthesis and characterization of Polymeric transition metal complexes with 1,10-phenanthroline and or Para-amino benzoate ligands 34 (Unpublished Master Thesis) Beirut Arab University, Beirut, Lebanon
25. Ishtiaque A, Rajendra P, Quraishi MA (2010) Adsorption and inhibitive properties of some new Mannich bases of Isatin derivatives on corrosion of mild steel in acidic media. Corros Sci 52:1472–1481
26. Shylesha BS, Venkatesha TV, Praveen BM (2011) Corrosion inhibition studies of mild steel by new inhibitor in different corrosive medium. Res J Chem Sci 1:46–50
27. Shinagawa T, Garcia-Esparza AT, Takanabe K (2015) Insight on Tafel slopes from a microkinetic analysis of aqueous electrocatalysis for energy conversion. Sci Rep 5:13801
28. Loto RT, Loto CA, Fedotova T (2014) Electrochemical studies of mild steel corrosion inhibition in sulfuric acid chloride by aniline. Res Chem Intermed 40:1501–1516
29. Salman HE, Balakit AA, Abdulridha AA, Makki SQ (2019) Synthesis of new aromatic azo-Schiff compound as carbon steel corrosion inhibitor in 1 M H_2SO_4; high efficiency at low concentration. IOP Conf Ser Mater Sci Eng 571:012077
30. Aoun SB, Bouklah M, Khaled KF, Hammouti B (2016) Electrochemical impedance spectroscopy investigations of steel corrosion in acid media in the presence of thiophene derivatives. Int J Electrochem Sci 11:7343–7358
31. Ghanbari A, Attar MM, Mahdavian M (2010) Corrosion inhibition performance of three imidazole derivatives on mild steel in 1 M phosphoric acid. Mater Chem Phys 124:1205–1209
32. Brug GJ, Van Den Eeden ALG, Sluyters-Rehbach M, Sluyters JH (1984) The analysis of electrode impedances complicated by the presence of a constant phase element. J Electroanal Chem 176:275–295
33. Tabesh RN, Abdel-Gaber AM, Hammud HH, Al-Oweini R (2019) Inhibition of steel corrosion in sulfuric acid solution by 1, 10-phenanthroline, para-aminobenzoate and their corresponding manganese complex. Z Phys Chem 233:1553–1569. https://doi.org/10.1515/zpch-2018-1254
34. Schweinsberg DP, Ashworth V (1988) The inhibition of the corrosion of pure iron in 0.5 M sulfuric acid by n-alkyl quaternary ammonium iodides. Corros Sci 28:539–545
35. Lagrenee M, Mernari B, Bouanis M, Traisnel M, Bentiss F (2002) Study of the mechanism and inhibiting efficiency of 3, 5-bis (4-methylthiophenyl)-4H-1, 2, 4-triazole on mild steel corrosion in acidic media. Corros Sci 44(3):573
36. Al-Moghrabi RS, Abdel-Gaber AM, Rahal HT (2018) A comparative study on the inhibitive effect of *Crataegus oxyacantha* and *Prunus avium* plant leaf extracts on the corrosion of mild steel in hydrochloric acid solution. Int J Ind Chem 9:255–263
37. Barranco V, Feliu S Jr, Feliu S (2004) EIS study of the corrosion behaviour ofzinc-based coatings on steel in quiescent 3% NaCl solution. Part 1: directly exposed coatings. Corros Sci 46:2203–2220
38. Langmuir I (1916) The constitution and fundamental properties of solids and liquids. Part I, solid. J Am Chem Soc 38:2221–2295
39. Florry P (1942) Thermodynamics of high polymer solutions. J Chem Phys 10:51–61
40. El-Awady A, Abd-El-Nabey B, Aziz S (1992) Kinetic- thermodynamic and adsorption isotherms analyses for the inhibition of the acid corrosion of steel by cyclic and open-chain amines. J Electrochem Soc 139:2149–2154
41. Abd-El-Nabey A, Abdel-Gaber A, Elawady G, El-Housseiny S (2012) Inhibitive action of some plant extracts on the alkaline corrosion of aluminum. Int J Electrochem Sci 7:7823–7839
42. Khalifa O, Abdallah S (2011) Corrosion inhibition of some organic compounds on low carbon steel in hydrochloric acid solution. Port Electrochim Acta 29:47–56
43. Cristofari G, Znini M, Majidi L, Bouyanzer A, Al-Deyab S, Paolini J, Hammouti B, Costa J (2011) Chemical composition and anti-corrosive activity of pulicaria mauritanica essential oil against the corrosion of mild steel in 0.5 M H_2SO_4. Int J Electrochem Sci 6:6699–6717
44. Ben Hmamou D, Salghi R, Zarrok H, Zarrouk A, Hammouti B, El Hezzat M, Bouachrine M (2012) Temperature effects on the corrosion inhibition of carbon steel in acidic solutions by Alizarin red. Adv Mater Corros 1:36–42
45. El-Etre AY, Ali AI (2017) A novel green inhibitor for C-steel corrosion in 2.0 mol L^{-1} hydrochloric acid solution. Chin J Chem Eng 25:373–380
46. Eddy N, Ebenso E (2008) Adsorption and inhibitive properties of ethanol extracts of musa sapientum peels as a green corrosion inhibitor for mild steel in H_2SO_4. Afr J Pure Appl Chem 2:46–54
47. Ashassi-Sorkhabi H, Shaabani B, Aligholipour B, Seifzadeh D (2006) The effect of some Schiff bases on the corrosion of aluminium in HCl solution. Appl Surf Sci 252:4039–4047
48. Lv G, Guo L, Qiu L, Yang H, Wang T, Liu H, Lin J (2015) Lipophilicity-dependent ruthenium N-heterocyclic carbene complexes as potential anticancer agents. Dalton Trans 44:7324
49. Tomaz AI, Jakusch T, Morais TS, Marques F, de Almeida RFM, Mendes F, Éva AE, Isabel S, João CP, Tamás K, Garcia MH (2012) [RuII(η5-C5H5)(bipy)(PPh3)]+, a promising large spectrum antitumor agent: cytotoxic activity and interaction with human serum albumin. J Inorg Biochem 117:261–269